

Characterization of sealed RPCs under strong irradiation source

Joana Pinto^{1,a}, Mário Carvalho^{1,b} and Telmo Paes^{1,2,c}

¹Universidade de Coimbra, Coimbra, Faculdade de Ciências e Tecnologias, Portugal

²Instituto Federal do Espírito Santo, Cariacica, Brazil

Project supervisor: Alberto Blanco Castro

October 1, 2024

Abstract. The gases used in Resistive Plate Chambers (RPCs) belong to the Hydro-fluorocarbons (HFCs) family, which greatly impact Global Warming. Because of this, we've been assisting to the implementation of strong restrictions on its use. To fight against this, sealed RPCs (sRPCs) are being developed. They do not need to have continuous gas flow or recycling gas systems. At the moment, it's not clear if this new line of detectors can substitute RPCs in all its fields of applications. However, they appear to be a valid option when the flux of particles is low (e.g. the natural flux of cosmic rays). In this work, we demonstrate the feasibility of operating a small area sRPC for tracking cosmic muons after 23 days of exposure to a intense radioactive source of gamma radiation without the need for gas replacement. A very intense radioactive source was used to simulate the detector's exposure to a typical lab exposure over a long period of time. The main characteristics of the sRPC were kept similar to a RPC with continuous gas flow: efficiency, average charge, and streamer percentage; without gas degradation.

KEYWORDS: sRPC, HFCs, RPCs, scintillators

1 Introduction

Resistive Plate Chambers, RPCs, are particle detectors whose sensible component is a gas. Their success is due to its excellent performance, high time resolution, and low construction cost. Because they're gaseous detectors, they rely on the purity of the gas in order to keep their performance stable. However, there's degradation of gas purity mainly from leaks and permeability in the system that allow atmospheric gases and humidity to enter and with the consequent release of HFCs (hydrofluorocarbons). This implies they need to have purification and cleaning systems. The release of HFCs are also harmful for the environment, increasing the greenhouse effect [1]. To mitigate this effect, RPCs that contain gas but are hermetically sealed after construction, called sRPC (sealed RPCs), have been developed[2].

1.1 Objective

This experiment aimed to test a sRPC to see if it performs as well as the typical RPCs without degradation or contamination of gas purity. For that, we analyzed the detector in terms of efficiency, charge, background and number of streamers, after prolonged exposure to a intense radioactive source, by studying the the response of the sRPC to flux of muons. We used a intense radiatioactive source to simulate the detector's exposure to typical laboratory radiation over a long period of time.

To achieve this, we started by assembling a structure to support the sRPC and four sintilators, connecting all the detector and Data AQUision (DAQ) components to a Front End Electronics board and a high voltage source.

Following some preliminary tests at LIP in Coimbra, we relocated the sytem to the "Laboratorio de radiofísica" in Santiago of Compostela to expose the detector to a in-entense radioactive 60-Cobalt source and collected data for subsequent analysis.

2 Setup and Operation

The experimental setup (Figure 1) consists of a sRPC module and a muon telescope, composed of four scintillators, placed behind the sRPC module. These are connected to a Data Acquisition (DAQ) system. The scintillators are used as reference counters to determine the sRPC response to cosmic-ray muons.

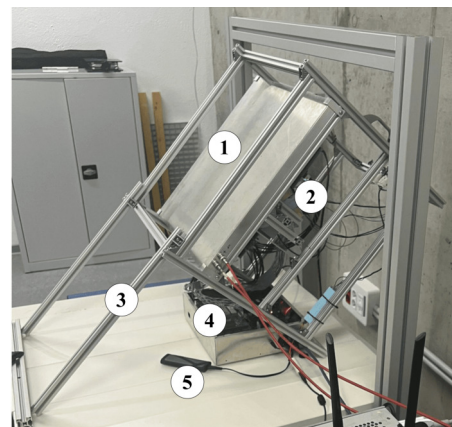


Figure 1: Assembly of setup detection sRPC with components: 1. sRPC; 2. SiPMs; 3. Aluminium Structure; 4. DAQ; 5. Extra Unity nVMe M.2 SSD.

^ae-mail: joana.carvalhoepinto@gmail.com

^be-mail: mario04daniel@gmail.com

^ce-mail: telmopbjunior@gmail.com

2.1 sRPC module

The tested sRPC module consist of a multi-gap structure [3] with two gaps, defined by three 2 mm thick soda lime glass electrodes, each measuring about 350 x 350 mm². Each gap includes a circular spacer, 1 mm thick, made of a soda lime glass disk (10 mm diameter) placed in the center of the active area and a strip (25 mm width), also made of soda lime glass, all around the periphery. The two gaps are filled with a mixture of 97.5% C₂H₂F₄ and 2.5% SF₆. The high-voltage (HV) electrodes are made of a semi-conductive layer based on acrylic paint, which is air-brushed onto the outer surface of the outermost glass electrodes. On top of the sRPCs is a FR4 layer with 16 copper strips with a pitch of 18 mm. Each strip is connected to the center conductor of a coaxial cable at each end, while the shielding is connected to a ground plane on bottom of the sRPC. Both ends are connected to high-speed Front End Electronics (FEE) [4].

The complete structure is enclosed in an aluminum box that provides the necessary electromagnetic insulation and mechanical rigidity. A sketch of the inner structure is provided in figure 2 and the interior of the sRPC in figure 3.

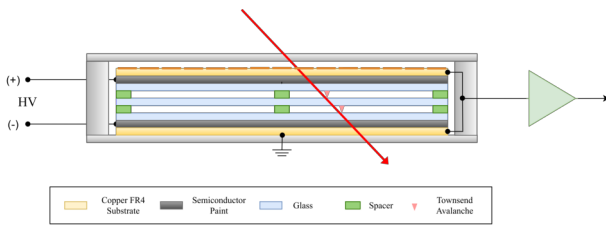


Figure 2: Sketch of the inner structure of the sRPC module.

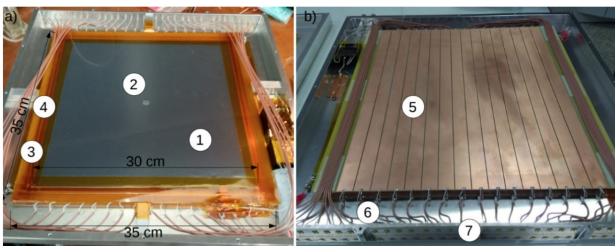


Figure 3: The interior of the sRPC. 1. HV layer, 2. Circular spacer in the center of the active area, 3. Strip spacer all around the periphery, 4. Mylar and Kapton layers, 5. Readout strip plane, 6. Coaxial cables and 7. MMCX RF feedthrough connectors.

2.2 Muon telescope

As shown in figure 4, the sRPC module was placed at 45° with the four scintillator, readout by SiPMs, placed in the back in a vertical position, forming a muon telescope. Styrofoam was added between the scintillators to decrease the

solid angle. With this arrangement, all the muons detected by the muon telescope pass through the sRPC module, guaranteeing the correct evaluation of the sRPC module efficiency.

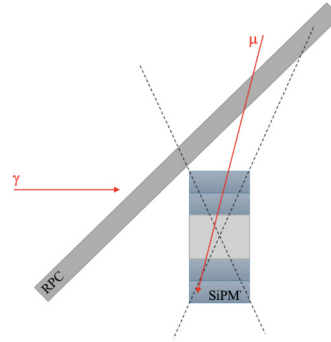


Figure 4: Sketch of the detector final setup.

2.3 Signals readout and Data Acquisition System

Fourteen out of sixteen strips of the sRPC module are connected to a FEE board [4]. The remaining two strips are grounded and not used. The four channel still available, on the FEE board, with the fast amplifier bypassed, are used to readout the SiPMs.

The resulting signals from the FEE board are processed by a Time Readout Board (TRB). Specifically the TRB3SC [5] version is used in this project. The TRB3SC board implements a 32-channel of Time-to-Digital Converter (TDC) embedded in an FPGA chip together with flexible logic providing the trigger.

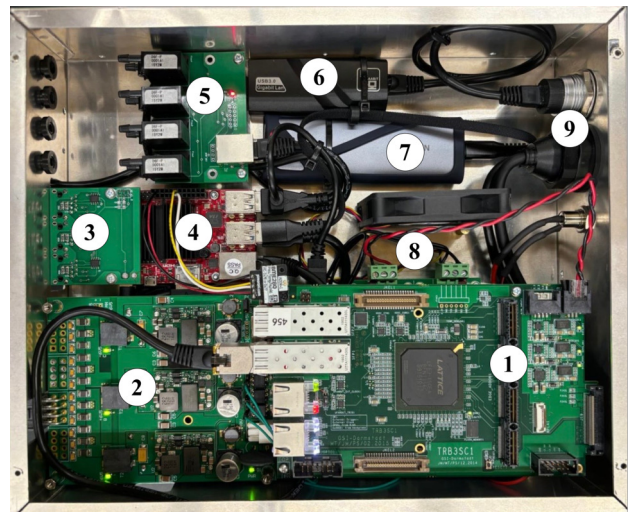


Figure 5: DAQ system and intern circuits: 1. FPGA Board TRB3SC1; 2. LV Power System; 3. I2C distribution board; 4. Mini-PC, 5. Gas Sensor Module, 6. USB Adapter Ethernet; 7. NVMe M.2 SSD; 8. Relay Control Board; 9. Power and computer connections..

3 Experimental Procedures

3.1 Charge, position (x,y) and time

The strips of the RPC are readout from both sides by the FEE, front and back. From these signals is possible to provide: the time T (leading edge of signal) with precision < 30 ps, and the charge Q (pulse width), the charge is obtained by measuring the Time over Threshold (T_{TOT}), on integrated (100) ns integration time) copy of the original signal.

The average front and back values ($(TF + TB)/2$ and $(QF + QB)/2$) correspond to the time and charge of the induced signal in each strip, respectively.

To determine the 2D position of a particle in the RPC, we assumed that the strip with the highest value of charge would be the assigned strip of the event, providing the position in the direction X . Having assigned a strip to the event, the transversal position Y can be computed using $(TF - TB)/2$ [6].

Figure 6 shows the results of the sRPC performance using $HV = 6kV$. In Figure 6a, we can see the number of all signals (hits) that the sRPC detects, and in Figure 6b, the average charge of these signals as a function of the position (X and Y).

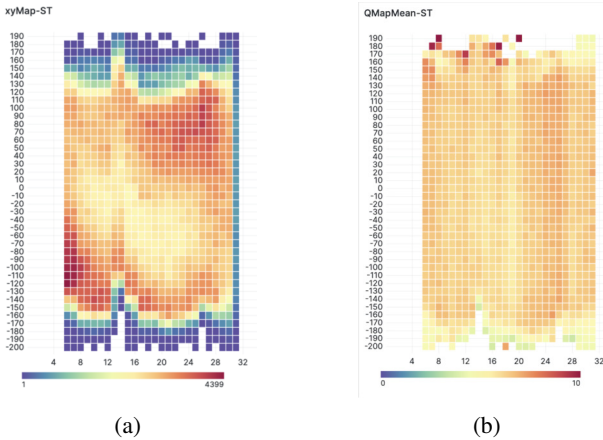


Figure 6: (a) Hits (b) average charge as a function of X and Y .

3.2 Muon filtering

To filter the coincidence signals from the scintillators so that they only corresponded to the passage of muons, it was necessary to analyze the coincidences in the presence of a gamma-radioactive source.

We collected several coincidence data points from the four scintillators, varying the position between the source and the SiPMs, and therefore the amount of gamma rays impinging the scintillators. We then obtained the blue curve in figure 7, where, as expected, the closer the source was to the SiPMs, the more events were detected. In order to remove the background signal corresponding to the gamma radiation, it was necessary to filter the signals measured.

So, we only accepted signals when: there were coincidences in the 4 scintillators, the signal width corresponding to the charge was larger than 240 ns and the time had a standard deviation of less than 2.5 ns.

With this filtering, we obtained the orange curve in figure 7 and 8, which shows that regardless of the proximity of the gamma-radioactive source, the number of true signals detected remained constant because it only depends on the muons that pass through the SiPMs.

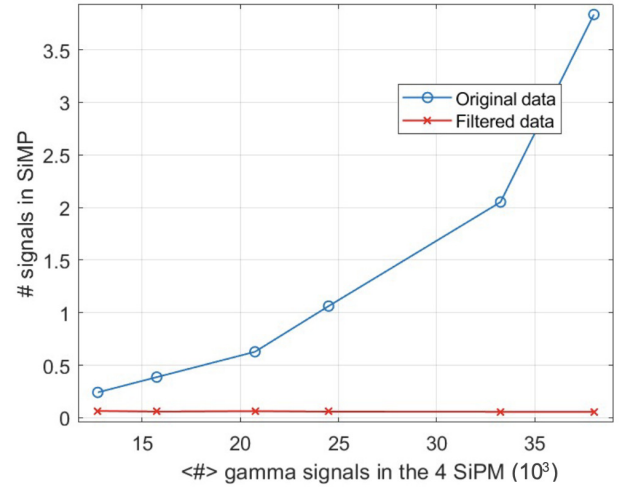


Figure 7: Comparison of the signals measured before and after gamma filtering in SiPMs.

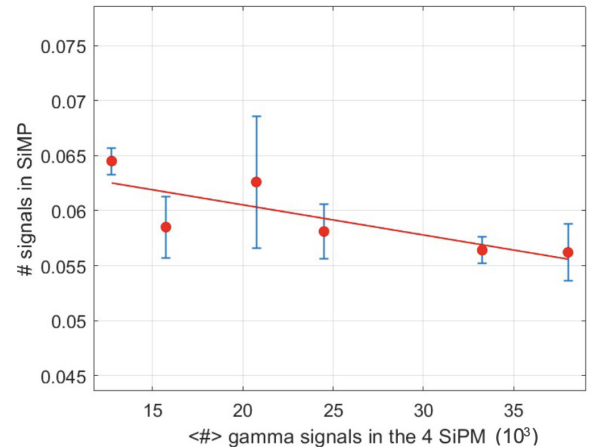


Figure 8: Signals from muons after the gamma filtering in SiPMs.

3.3 High Voltage Efficiency

To determine the operational high voltage to use in this setup, we tested the sRPC with different voltages, and the efficiency (ϵ) was calculated as shown in equation 1. These data were combined in figure 9, where we can see that the sRPC reaches a plateau (relatively steep) above

95% for voltages above 6kV. The Operational High Voltage was, therefore, set to 6kV.

$$\varepsilon (\%) = \frac{\# \text{ events in RPC}}{\# \text{ events in 4 Scintillators}} \times 100 \quad (1)$$

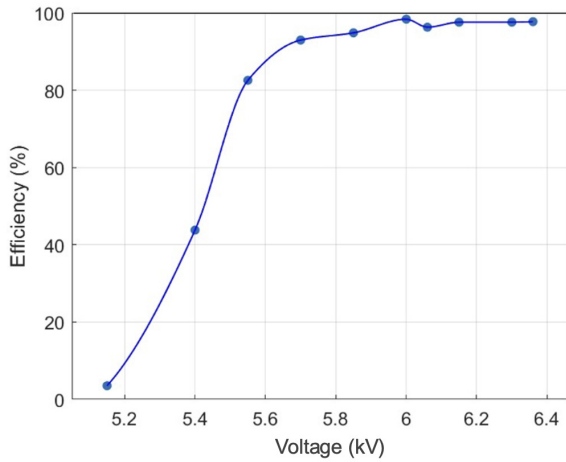


Figure 9: Efficiency as a function of voltage.

We analyzed the detector performance using the trigger based on the scintillator telescope. This means that we only considered events in the sRPC that passed through all four scintillators.

In figure 10a, we can see the number of signals (hits) that the sRPC detects using the muon filter, and in figure 10b, the average charge of these detections as a function of the position (X and Y). In both plots, we can see that the particles detected are localized in just one region of the sRPC. This region corresponds to the position of the telescope behind the sRPC.

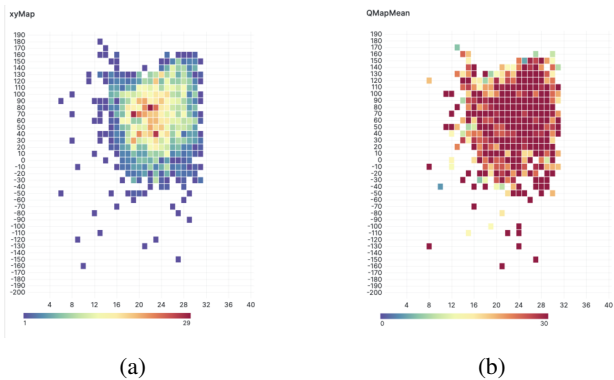


Figure 10: Particle distribution in the sRPC using muon-Trigger (a) Particle hits (b) average charge as a function of X and Y.

4 Tests: Exposing the detector to a intense radiation

To test the sRPC, we exposed the detector for 20 days under a intense radioactive (Cobalt-60) source at "Laboratorio de radiofísica" in Santiago of Compostela. The initial plan was to collect cosmic rays using the muon trigger continuously throughout the entire experiment (with the source active 24/7). However, the radiation from the source was too intense, and even after attempting to attenuate it with several lead plates, the sRPC (being highly sensitive to any radiation) became saturated, making it impossible to collect muon signals. The solution was to irradiate the sRPC for 20 hours and then turn it off for the remaining 4 hours each day. During these 4 hours, we were able to run the muon trigger and compare the collected data over the course of several days.

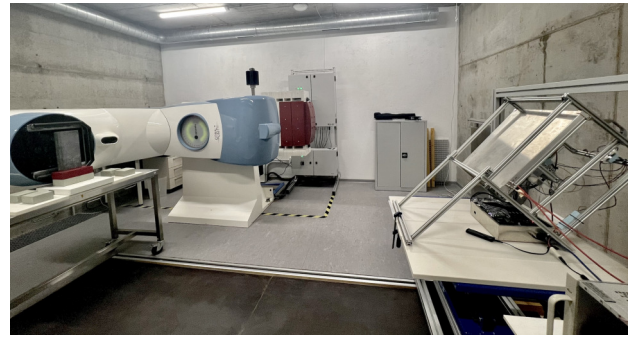


Figure 11: Detector at "Laboratorio de Radiofísica" in Santiago of Compostela in front of a intense radioactive source.

5 Results

The data from the 23 days of experience at Santiago's Laboratory is combined in figure 12. The first row corresponds to the HV current, when the current equals to zero that means that the radioactive source was turned off and we ran the muons trigger. In this intervals of time (4h/day) we analyzed the rate, charge, the number of streamers and efficiency because all of them are very sensitive to the quality of the gas.

- $\langle Q \rangle$: average charge of signals
- %Streamers: number of events above a certain level.
- Eff: efficiency of the sRPC,
- Background: number of signals generated without a radioactive source

The efficiency, figure13, average charge, figure 14, and the percentage of streamers, figure 15, remained stable throughout the period of irradiation and also after the 23 days. For the background, as we can see in figure 16, it started to rise at first and then stabilized again. This could be related to some external factor and not to the gas degradation because it was stable even after some days of irradiation .

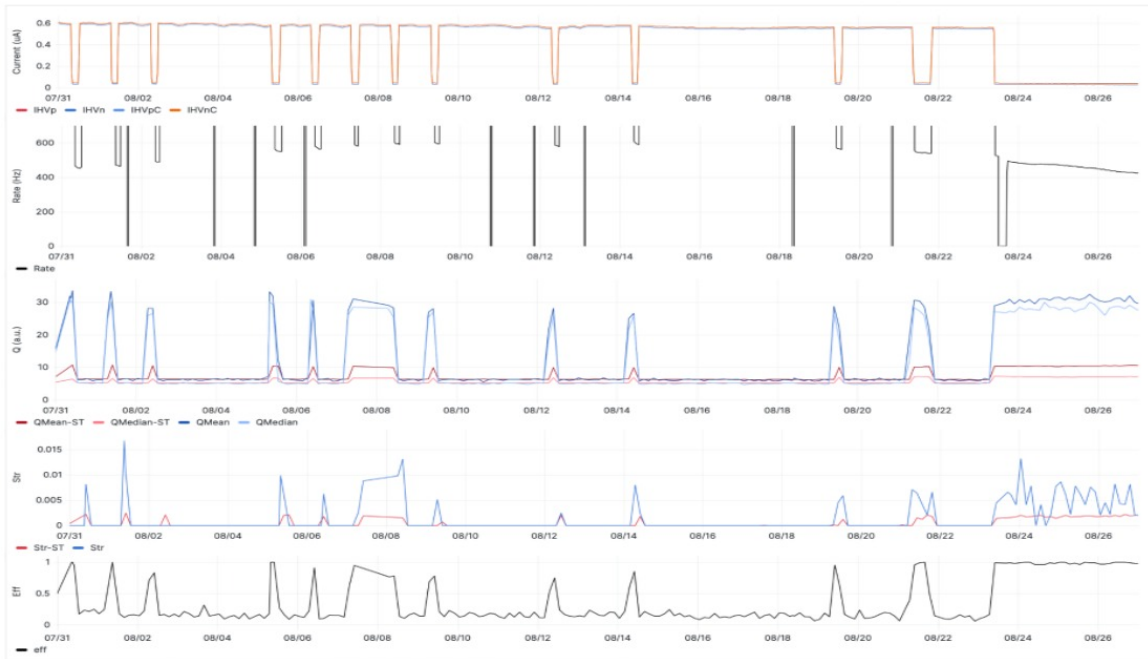


Figure 12: Results exposing the detector to an intense radioactive source.

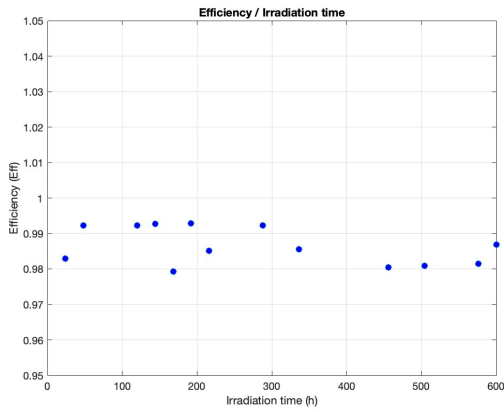


Figure 13: Efficiency as function of irradiation time.

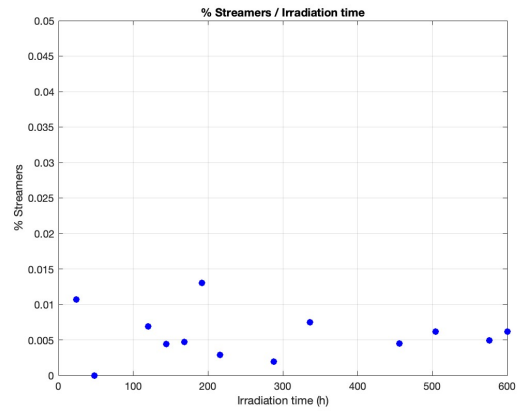


Figure 15: %streamers as function of irradiation time.

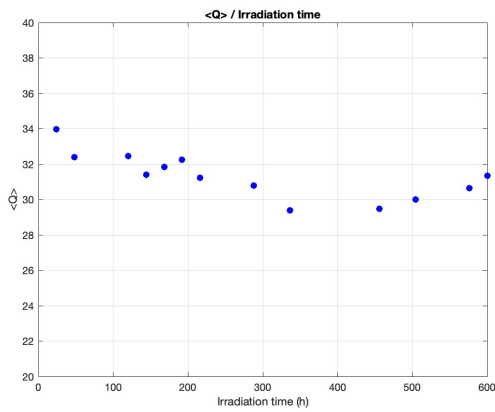


Figure 14: $\langle Q \rangle$ as function of irradiation time.

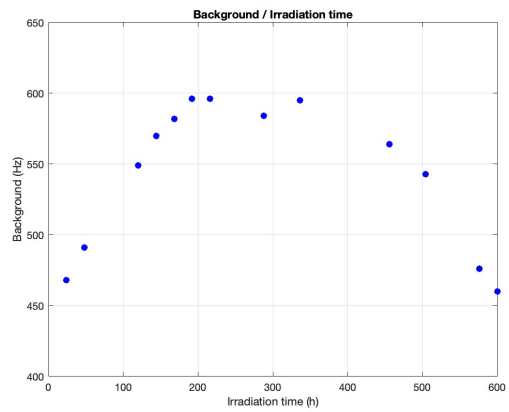


Figure 16: Background as function of irradiation time.

6 Conclusions

After almost a month, efficiency varied between 98% and 100%. Thus, the efficiency remains high and the percentage of streamers is low. The results indicate the feasibility of operating a sRPC for long periods of exposure without the need of gas replacement when exposed to the flow of natural cosmic rays and intense source of gamma radiation, as seen in Santiago.

Acknowledgements

We're sincerely grateful to our supervisor, Alberto Blanco Castro, and the entire team at LIP for the enriching summer internship. Thank you for their guidance and support. This experience has shaped our future positively. We also want to thank the staff at "Laboratorio de radiofísica" of Santiago of Compostela University for all the support and disponibility.

References

- [1] B. Mandelli, "Eco-gas mixtures and mitigation procedures for green-house gases (ghgs)," in *ECFA Detector R&D Road-map Symposium: TF*, vol. 1, 2021.
- [2] A. Blanco, P. Fonte, L. Lopes, and M. Pimenta, "Sealed (zero gas flow) resistive plate chambers," *The European Physical Journal Plus*, vol. 138, no. 11, p. 1021, 2023.
- [3] E. C. Zeballos, I. Crotty, D. Hatzifotiadou, J. L. Valverde, S. Neupane, M. Williams, and A. Zichichi, "A new type of resistive plate chamber: the multi-gap rpc," *Nuclear Instruments and Methods in Physics Research Section A: Accelerators, Spectrometers, Detectors and Associated Equipment*, vol. 374, no. 1, pp. 132–135, 1996.
- [4] D. Belver, P. Cabanelas, E. Castro, J. A. Garzón, A. Gil, D. Gonzalez-Diaz, W. Koenig, and M. Traxler, "Performance of the low-jitter high-gain/bandwidth front-end electronics of the hades trpc wall," *IEEE Transactions on Nuclear Science*, vol. 57, no. 5, pp. 2848–2856, 2010.
- [5] G. Korcyl, L. Maier, J. Michel, A. Neiser, M. Palka, M. Penschuck, P. Strzempek, M. Traxler, and C. Ugur, "A users guide to the trb3 and fpga-tdc based platforms," 2015.
- [6] M. Xarepe, T. Aumann, A. Blanco, A. Corsi, D. Galaviz, H. Johansson, S. Linev, B. Löher, L. Lopes, J. Michel, *et al.*, "Resistive plate chambers for precise measurement of high-momentum protons in short range correlations at r3b," *Nuclear Instruments and Methods in Physics Research Section A: Accelerators, Spectrometers, Detectors and Associated Equipment*, vol. 1055, pp. 168–445, 2023.